

Resonance Raman and Fourier Transform Infrared Detection of Azide Binding to the Binuclear Center of Cytochrome *bo*₃ Oxidase from *Escherichia coli*

Constantinos Varotsis* and Magdalini Vamvouka

University of Crete, Department of Chemistry, 71409 Iraklion, Crete, Greece

Received: November 18, 1998; In Final Form: February 10, 1999

Resonance Raman and FTIR spectra are reported for the oxidized azide-bound derivative of the quinol cytochrome *bo*₃ oxidase from *Escherichia coli*. The resonance Raman spectra display three isotope-dependent vibrational modes at 419, 2040, and 2061 cm⁻¹. The FTIR spectra display two isotope-dependent bands at 2040 and 2061 cm⁻¹. We assign the band at 419 cm⁻¹ to $\nu(\text{Fe}-\text{N}_3-\text{Cu}_\text{B})$ and the bands at 2040 and 2061 cm⁻¹ to $\nu_\text{as}(\text{N}_3)$. The observation of two $\nu_\text{as}(\text{N}_3)$ modes suggests that the azide ion binds to two different enzyme conformations, both forming bridging complexes with the binuclear center. Comparison of the FTIR data of the azide-bound cytochrome *bo*₃ and cytochrome *aa*₃ complexes reveal that there are quantitative differences in the structure of the heme *o*₃-Cu_B and heme *a*₃-Cu_B binuclear pockets upon azide binding. The present data on the vibrational frequencies of the azide-bound cytochrome *bo*₃ complex do not support the recent proposal that azide binds as a terminal ligand to Cu_B (Little, R. H.; Cheesman, M. R.; Thomson, A. J.; Greenwood, C.; Watmough, N. J. *Biochemistry* **1996**, *35*, 13780–13787) but are more reasonably interpreted to conclude that azide functions as a bridge between heme *o*₃ and Cu_B.

Cytochrome *bo*₃, the terminal oxidase in the aerobic respiratory chain of *Escherichia coli*, catalyzes the transfer of electrons from ubiquinol-8 to O₂.^{1–21} Members of the quinol heme–copper oxidase family, including cytochrome *bo*₃, lack the EPR-visible copper center, which is typical of the cytochrome *c* oxidase (CcO).^{1,10,11} Accordingly, this enzyme contains only three redox active metal sites: a low-spin heme *b*, which is involved in electron transfer and a high spin heme *o*₃, which forms a heme–copper binuclear catalytic site. Although there are notable differences between CcO and quinol cytochrome *bo*₃, including the lack of the dinuclear Cu_A center and the electron-donating substrate, cytochrome *bo*₃ exhibits the two chemically distinct but functionally related catalytic activities known to all heme–copper oxidases.^{7–10} That is, it functions as a proton pump and reduces dioxygen through intermediates that are similar to those found in the cytochrome *c* oxidase/O₂ reaction.²²

The properties of the oxygen-binding environment in heme–copper oxidases have been studied by examining the coordination of small ligands to the binuclear center, in particular those that form stable reduced heme-bound complexes, by resonance Raman (RR) and FTIR spectroscopies.^{23,24} With this approach the CO-sensitive modes in cytochrome *bo*₃ were identified by Wang et al.^{23a} and found to be similar to those of the CO-bound CcO complex.²⁴ Accordingly, it was suggested that the bacterial and mammalian enzymes have similar binuclear centers.^{23b} Several spectroscopic studies of ligand binding to oxidized cytochromes *aa*₃ and *bo*₃ have been reported. However, a general conclusion based on these reports was difficult to formulate because a complete vibrational study of liganded oxidized cytochromes *aa*₃ and *bo*₃ is lacking.^{25–27} The assignment of the azide-sensitive modes, which have been detected by FTIR spectroscopy in both cytochromes *aa*₃ and *bo*₃ oxidase

have been a conundrum and subject of debate for a number of years. A number of chemically interesting structures have been suggested for azide-bound mammalian CcO and cytochrome *bo*₃.^{26,28–31} Yoshikawa and Caughey²⁵ used FTIR spectroscopy and observed two azide-sensitive modes with $\nu_\text{asym} = 2051 \text{ cm}^{-1}$ and $\nu_\text{asym} = 2038 \text{ cm}^{-1}$, which they attributed to azide binding within the protein moiety near the binuclear site and to Cu_B, respectively. Later, Tsubaki²⁶ with the same approach of Yoshikawa and Caughey²⁵ argued that the 2051 cm⁻¹ mode arises from a bridging structure between heme *a*₃ and Cu_B, and the 2039 cm⁻¹ mode from a high-spin ferric heme *a*₃-azide species.²⁶ More recently, Li and Palmer interpreted their FTIR, EPR, and MCD data to assign the 2039 cm⁻¹ mode to azide bound to heme *a*.³⁰ Unfortunately, these three studies have failed to agree on the mode of azide binding to mammalian CcO. In cytochrome *bo*₃ Tsubaki et al.³¹ suggested that the 2041 cm⁻¹ mode observed in their FTIR spectra arises from the asymmetric stretch of the bridge between the heme *o*₃ and Cu_B azide molecule. Little et al.,²⁸ however, reported that azide binds as a terminal ligand to Cu_B and yields a binuclear center in the form Fe(III)–OH₂Cu_B–N₃.

Because most of the proposed mechanisms for the translocation of protons by the heme–copper oxidases involve ligand rearrangement around the heme–Cu_B center³² and since there are conflicting data regarding the azide-binding to the binuclear center of cytochrome *bo*₃,^{28,31} we have reexamined the FTIR spectra of the N₃-bound cytochrome *bo*₃ complex and compare them with those of the azide-bound CcO complex. Moreover, we have used RR spectroscopy to probe the heme *o*₃ moiety upon azide-binding and found three azide-sensitive modes located at 419, 2040, and 2061 cm⁻¹. The FTIR data of the azide-bound cytochrome *bo*₃ and CcO complexes showed two azide-sensitive modes: a major mode at 2040 cm⁻¹ and a minor mode at 2061 cm⁻¹, in the cytochrome *bo*₃–N₃ complex, and a minor mode at 2041 cm⁻¹ and a major mode at 2050 cm⁻¹, in the CcO–N₃ complex. Our data indicate that the azide-

* Corresponding author. Fax: 30-81-210951. E-mail: varotsis@chemnt.chemistry.ucl.gr.

sensitive modes observed at 419 cm^{-1} in the RR spectra, and at 2040 and 2061 cm^{-1} in both the RR and FTIR spectra, arise from $\nu(\text{Fe}-\text{N}_3-\text{Cu}_\text{B})$ and $\nu_{\text{as}}(\text{N}_3)$, respectively, of the heme *o*₃ $\text{Fe}-\text{N}=\text{N}=\text{N}-\text{Cu}_\text{B}$ complex. These assignments suggest that azide binds to two different enzyme conformational states, both forming bridging complexes with the heme *o*₃- Cu_B binuclear center and still preserving the high-spin characteristics of the heme *o*₃ center and the spin coupling of the binuclear center metals. Comparison of the FTIR data of the azide-bound complexes of cytochrome *bo*₃ and CcO reveal that the affinity of the species that gave the two distinct asymmetric azide stretching modes at 2061 and 2040 cm^{-1} in the cytochrome *bo*₃- N_3 complex is reversed in the analogous complex of CcO. In addition, the frequency of the 2061 cm^{-1} asymmetric mode observed in cytochrome *bo*₃ is 10 cm^{-1} higher than the corresponding mode found in CcO. This observation indicates that there are quantitative differences in the structure of the oxidized heme *o*₃- Cu_B and heme *a*₃- Cu_B binuclear pockets upon azide binding.

Materials and Methods

Cytochrome *bo*₃ from *E. coli* was isolated by the procedure published previously.¹⁰ The enzyme was solubilized in 100 mM Tris-HCl buffer at pH 7.6 with 0.05% dodecyl β -D-maltoside. The azide-bound enzyme was prepared by incubating the oxidase in 600 μM NaN_3 overnight. Resonance Raman spectra were obtained from 30–40 μM samples, pH 7.6, in a cylindrical quartz spinning cell maintained at 3–5 $^\circ\text{C}$ by a stream of cold nitrogen gas. The Raman spectra were acquired by using a SPEX 1877 triplemate with an EG&G (model 1530-CUV-1024S) CCD detector. A Coherent Innova K-90 krypton ion laser was used to provide the excitation wavelength of 413.1 nm. The power incident on the oxidase samples was typically 8–10 mW. FTIR spectra were recorded from 200 to 250 μM samples at 2 cm^{-1} resolution with a Bruker Equinox 55 FTIR spectrometer equipped with a liquid nitrogen cooled mercury cadmium telluride detector. The azide-bound samples were loaded into a cell with CaF_2 windows and a 0.052 mm spacer. An average of 2000 scans was used for each spectrum. Optical absorption spectra were recorded before and after FTIR and Raman measurements in order to assess sample stability with a Perkin-Elmer Lambda 20 UV-visible spectrophotometer.

Results and Discussion

The optical absorption spectra of oxidized and azide-bound cytochrome *bo*₃ are shown in Figure 1. Addition of azide causes a small shift in the Soret maximum from 408 to 410 nm and small intensity changes at 532 and 562 nm. This implies that heme *o*₃ remains six-coordinate high-spin following azide binding, as previously reported by EPR and MCD spectroscopies.²⁸

The RR technique is a powerful method to probe heme structures and yields data on the spin state and coordination state of the iron atom of these chromophores that complement insights available from FTIR and EPR spectroscopies.³³ Figure 2A shows the high-frequency RR spectrum of oxidized cytochrome *bo*₃, and that of the $^{14}\text{N}_3$ -bound cytochrome *bo*₃ is presented in Figure 2B. The principal modes presented in Figure 2A at 1374 (ν_4), 1478 (ν_3), 1580 (ν_2), and 1630 cm^{-1} (ν_{10}) firmly establish the presence of the six-coordinated high-spin heme *o*₃.^{23b} Also present in this spectrum are modes at 1505 (ν_3) and 1641 cm^{-1} (ν_{10}), indicating the presence of the six-coordinated ferric, low-spin heme *b*.^{23b} Upon conversion of the enzyme to the N_3 -bound form, the frequencies and the intensities of the

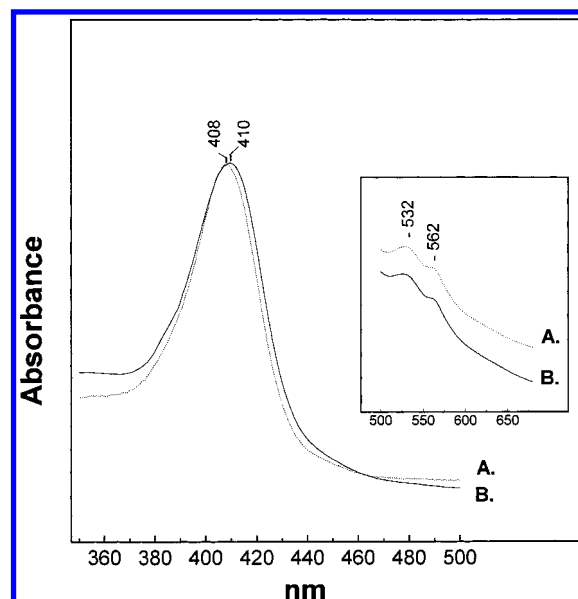


Figure 1. Optical absorption spectra of oxidized cytochrome *bo*₃ (Figure 1A) and the azide-bound cytochrome *bo*₃ (Figure 1B). All spectra were recorded in a 0.5 cm path length at 25 $^\circ\text{C}$. The enzyme was diluted to a final concentration of 5.5 μM in 50 mM Hepes and 0.3% dodecyl β -D-maltoside at pH 7.4.

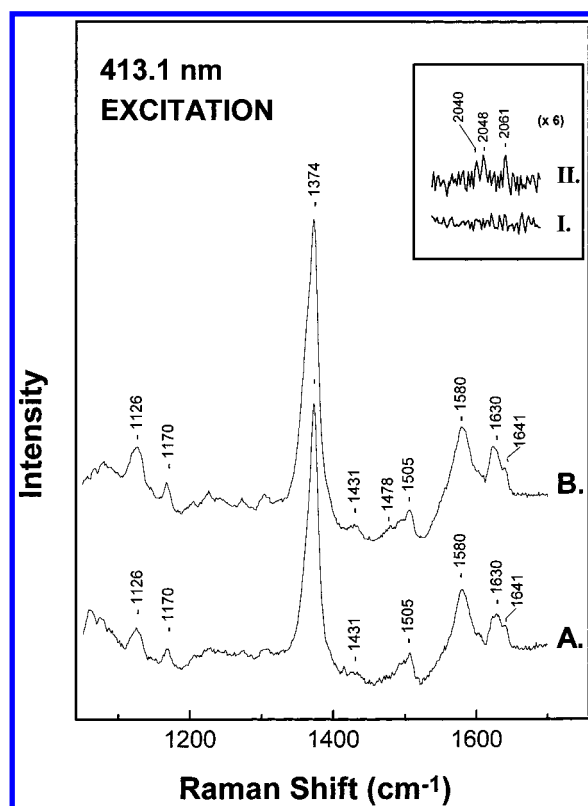


Figure 2. High-frequency resonance Raman spectra of (A) oxidized cytochrome *bo*₃ and (B) the $^{14}\text{N}_3$ -bound complex of cytochrome *bo*₃. Inset: oxidized (trace I) and $^{14}\text{N}_3$ -bound cytochrome *bo*₃ (trace II) in the 2000–2080 cm^{-1} region. The exciting laser frequency was 413.1 nm.

RR skeletal modes of heme *o*₃ and heme *b* remain similar to those found in the RR spectrum of the oxidized enzyme. This indicates that heme *o*₃ remains six-coordinate high-spin and heme *b* six-coordinate low-spin upon azide binding. The spectral region where the $\nu_{\text{as}}(\text{N}_3)$ vibrations are expected to occur is shown in the inset in Figure 2. Spectrum I is that of the oxidized enzyme and spectrum II that of the $^{14}\text{N}_3$ -bound form. There are

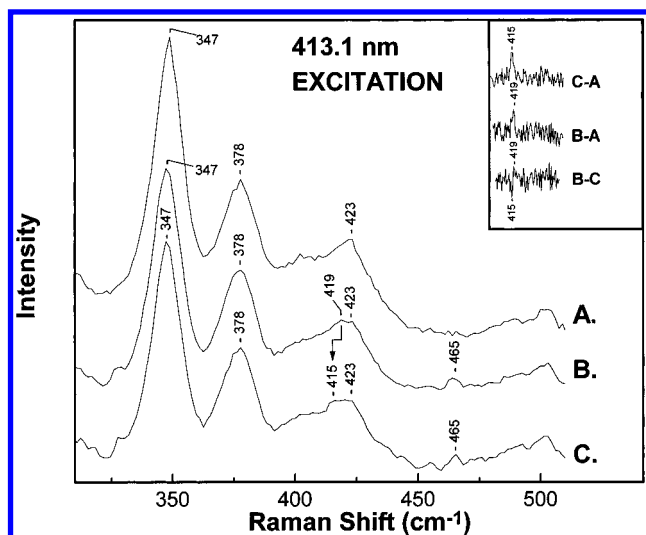


Figure 3. Low-frequency resonance Raman spectra of (A) oxidized cytochrome *b*_{o3}, (B) the ¹⁴N₃-bound complex of cytochrome *b*_{o3}, and (C) the ¹⁵N¹⁴N₂-bound complex of cytochrome *b*_{o3}. The exciting laser frequency was 413.1 nm.

three new modes located at 2041, 2048, and 2061 cm⁻¹ in the spectrum of the N₃-bound form. The 2048 cm⁻¹ mode is due to free N₃. The frequencies of the 2040 and 2061 cm⁻¹ RR modes are very close to those that have been observed in the FTIR spectra of the N₃-bound cytochrome *b*_{o3} by Tsubaki et al.³¹ This finding, in conjunction with the FTIR data, suggests that N₃ is bound to heme *o*₃. Direct confirmation of this hypothesis requires detection of the iron heme *o*₃³⁺-N₃ vibration.

Figure 3A shows the low-frequency RR spectrum of oxidized cytochrome *b*_{o3}, and those of the ¹⁴N₃-bound and the ¹⁵N₃-bound cytochrome *b*_{o3} are given in Figure 3B,C, respectively. The principal bands seen in Figure 3 located at 347, 378, and 423 cm⁻¹ have contributions from both heme *b* and heme *o*₃. Spectrum B (¹⁴N₃) is similar to spectrum A with the exception that a new mode appears at 419 cm⁻¹. Spectrum C shows that the 419 cm⁻¹ mode in the ¹⁵N¹⁴N₂ spectrum is downshifted to 415 cm⁻¹ when the experiment is repeated with ¹⁵N¹⁴N₂. The frequency of this mode and the 4 cm⁻¹ isotope shift allows us to assign it as the heme *o*₃ Fe-N₃ stretching vibration in the cytochrome *b*_{o3}-N₃ complex. The difference spectra shown in the inset further support our assignment of the 419 cm⁻¹ mode as arising from the heme *o*₃ Fe-N=N=N-Cu_B species. The difference spectra C-A and B-A are obtained by subtracting the Raman spectrum of the resting enzyme from that of the enzyme reacted with ¹⁵N¹⁴N₂ and ¹⁵N¹⁴N₂, respectively. The modes located at 419 and 415 cm⁻¹ and the 419 cm⁻¹ peak/415 cm⁻¹ trough pattern shown in the difference spectrum B-C indicate that the 419 cm⁻¹ mode is an azide-isotope-sensitive RR mode. The fact that such spectra were obtained from several independent preparations makes the presence of the azide-isotope-sensitive band reliable. Two stretching vibrations should be observed because of the 1:1 ratio of the Fe-N₂¹⁵N-Cu_B and Fe-¹⁵NN₂-Cu_B groups present in the sample with the terminally labeled sodium azide (Na¹⁵NN₂). Obviously, the spectral resolution is not high enough to separate these bands and instead we observed a broad band at 415 cm⁻¹.

The most reasonable assignment of the 419 cm⁻¹ stretching vibration is that it arises from a heme *o*₃-N=N=N-Cu_B complex. Although the frequency of the heme *o*₃-N₃ mode is very close to that reported for Mb-N₃^{34,35} and Hb-N₃,^{36,37} our combined RR and FTIR data (see below) and the isotope shift

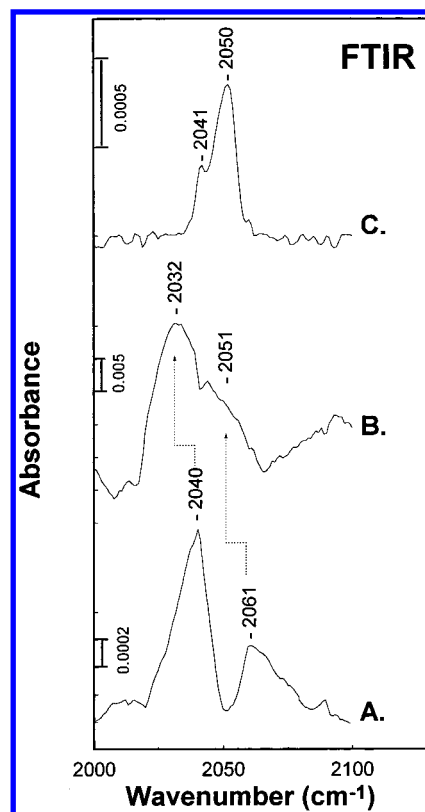


Figure 4. FTIR spectra of (A) oxidized ¹⁴N₃-bound cytochrome *b*_{o3}, (B) oxidized ¹⁵N¹⁴N₂-bound cytochrome *b*_{o3}, and (C) oxidized ¹⁴N₃-bound mammalian cytochrome *aa*₃.

we detect are most consistent with a model in which Cu_B has a direct interaction with the bound azide group. The precise extent of the azide isotope shift is important because it is sensitive to the coordination of the azide. The small isotope shift we detect of 4 cm⁻¹ for the ¹⁴N₃/¹⁵N¹⁴N₃ exchange, when compared to the 7 cm⁻¹ shift observed in Mb-N₃, Hb-N₃, and other azidoiron porphyrin complexes,³⁸ suggests that the azide molecule is not terminally bound to the iron heme *o*₃ but it is rather bridged between the two metal centers (Fe-N₃-Cu_B). Thus, our data do not support the conclusions of Little et al.²⁸ that, in binding at the binuclear site, azide is terminally bound to Cu_B.

Fourier transform infrared (FTIR) spectroscopy has been used to monitor and characterize not only the binding and dynamics of ligands bound to heme *o*₃ but also ligands bound to Cu_B.³⁹ To facilitate such assignments, we have obtained the FTIR spectra of the azide-bound cytochrome *b*_{o3} under the same enzyme:azide concentrations as we used in the RR experiments.

The FTIR spectrum of the ¹⁴N₃-bound cytochrome *b*_{o3} shown in Figure 4A exhibits bands at 2061 and 2040 cm⁻¹, both of which display azide isotopic sensitivity by shifting to 2051 and 2032 cm⁻¹, respectively, in the ¹⁵N¹⁴N₂ derivative (trace B). Spectrum C is that of the ¹⁴N₃-bound CcO. Comparison of spectrum A with spectrum C shows that similar results are obtained for azide-bound CcO. There are, however, some clear differences. The 2061 cm⁻¹ mode is 10 cm⁻¹ higher in cytochrome *b*_{o3} than it is in CcO, and there is no splitting of the 2061 cm⁻¹ mode in the ¹⁵N¹⁴N₂ experiment. The latter observation indicates that the strength of the two internal N=N bonds are very similar to each other. A splitting on the order of 9 cm⁻¹ has been observed for the 2050 cm⁻¹ mode in the ¹⁵N¹⁴N₂ experiment for CcO.³⁰ Thus, the frequency differences between the azide-isotope-sensitive modes in cytochrome *b*_{o3} and CcO indicate that the binuclear site of cytochrome *b*_{o3}, while

similar, is not identical to its mammalian counterpart upon azide binding. The frequency of the 2040 cm⁻¹ mode in cytochrome *bo*₃ is close to that observed for the high-spin Mb-N₃^{40,41} and azidoiron porphyrins³⁸ and the same as that previously reported by Tsubaki et al.³¹ for the cytochrome *bo*₃-N₃ complex. These authors³¹ assigned the 2040 cm⁻¹ mode to the asymmetric stretch of the bridging azide on the basis of the observation that it could be replaced with a minimum amount of cyanide, producing the heme *o*₃-C-N-Cu_B bridging complex characterized by the 2146 cm⁻¹ mode, and therefore the azide ion must occupy the same or overlapping site with this bridging cyanide; our data (not shown) confirm their results.

While we are unable to assess unambiguously the nature of the minor component with frequency at 2061 cm⁻¹, we propose that it can be attributed to one of two different adducts, one of which is Cu_B-N₃. The 2056 cm⁻¹ frequency for the Cu_B adduct is similar to that reported by Blackburn et al.⁴² for Cu_B-N₃ of superoxide dismutase and close to that we have observed for Cu-N₃ of nitrite reductase (Varotsis et al. unpublished results). The second adduct arises from a distinct enzyme conformation, which is described by the 419 and 2061 cm⁻¹ modes, the former being related to the 419 and 2040 cm⁻¹ modes, within the heme *o*₃-Cu_B binuclear center. Therefore, of the two possible interpretations outlined above we favor the second in which the azide ion binds to two different conformational states, both having bridging structures. This can also explain why the bridging ligand cyanide displaces azide from its binding site.

The frequencies and intensities of the asymmetric azide stretches, as well as the correlation between them, are of great help in the determination of the binuclear center environment of the azide adducts and therefore allow inferences concerning possible structures of the catalytic site of the heme-copper oxidases to be made. Although the azide modes have not been unequivocally assigned for CcO, comparison of the spectra shown in Figure 4A,C reveals that the intensity ratio of the high-frequency 2050 cm⁻¹/low-frequency 2041 cm⁻¹ modes in CcO is reversed in cytochrome *bo*₃. In cytochrome *bo*₃, the intensity of the high-frequency 2061 cm⁻¹ mode is lower than that of the low-frequency 2040 cm⁻¹ mode. Equivalent differences have not been reported in other coordination or oxidation states of CcO and cytochrome *bo*₃. Such differences can be attributed to changes in the distal environment, such as a change in the position of Cu_B. Therefore, it will be interesting to determine if there are associated variations in the catalytic function between CcO and cytochrome *bo*₃, since the interaction of Cu_B and its ligand set with the heme-bound oxygen intermediates could be different for these two terminal oxidases.

The present resonance Raman and FTIR data provide clear evidence for the controversial assignment of the azide molecule binding in the binuclear center of cytochrome *bo*₃. The 419 and 2040 cm⁻¹/2061 cm⁻¹ modes are assigned to the stretching mode and asymmetric stretching mode of the heme *o*₃-N=N-Cu_B complex. Moreover, we attribute the observed different intensity ratio of the high-frequency/low-frequency azide modes in cytochrome *bo*₃, as compared to CcO, to an apparent difference in the azide-binding affinity between the bacterial and mammalian enzymes. The redox-linked conformational changes at the heme *o*₃-Cu_B binuclear center upon azide binding to partial reduced forms of the enzyme is under investigation.

Acknowledgment. We are indebted to Prof. Gerald Babcock for the use of the LASER laboratory facility at Michigan State University and to Prof. M. Wikström and Dr. A. Puustinen for supplying the cytochrome *bo*₃ samples. This work was supported

by Alexander von Humboldt-Stiftung, DFG (SFB 472), Fonds der Chemischen Industrie, a NATO grant (GRG 940275), and PENED-95.

References and Notes

- (1) Anraku, Y.; Gennis, R. B. *Trends Biochem. Sci.* **1987**, *12*, 262-266.
- (2) Chepur, V.; Lemieux, L.; Au, C. C.-T.; Gennis, R. B. *J. Biol. Chem.* **1990**, *265*, 11185-11192.
- (3) Miller, M. J.; Gennis, R. B. *J. Biol. Chem.* **1983**, *258*, 9159-9165.
- (4) Bolgiano, B.; Salmon, I.; Ingledew, W. J.; Poole, R. K. *Biochem. J.* **1991**, *274*, 723-730.
- (5) Minagawa, J.; Mogi, T.; Gennis, R. B.; Anraku, Y. *J. Biol. Chem.* **1992**, *267*, 2096-2094.
- (6) Kita, K.; Kasahara, M.; Anraku, Y. *J. Biol. Chem.* **1982**, *257*, 7933-7935.
- (7) Puustinen, A.; Finel, M.; Virkki, M.; Wikström, M. *FEBS Lett.* **1989**, *249*, 163-167.
- (8) Puustinen, A.; Finel, M.; Haltia, T.; Gennis, R. B.; Wikström, M. *Biochemistry* **1991**, *30*, 3936-3942.
- (9) Puustinen, A.; Morgan, J. E.; Verkhovsky, M.; Thomas, J. W.; Gennis, R. B.; Wikström, M. *Biochemistry* **1992**, *31*, 10363-10369.
- (10) Puustinen, A.; Wikström, M. *Proc. Natl. Acad. Sci. U.S.A.* **1991**, *88*, 6122-6129.
- (11) Saraste, M.; Holm, L.; Lemieux, L.; Lübbers, M.; van der Oost, J. *Biochem. Soc. Trans.* **1991**, *19*, 608-612.
- (12) Wu, W.; Chang, C. K.; Varotsis, C.; Babcock, G. T.; Puustinen, A.; Wikström, M. *J. Am. Chem. Soc.* **1992**, *114*, 1182-1187.
- (13) Gohlke, U.; Warne, A.; Saraste, M. *EMBO J.* **1997**, *16*, 1181-1188.
- (14) Calhoun, M. W.; Hill, J. J.; Lemieux, L. J.; Ingledew, W. J.; Alben, J. O.; Gennis, R. B. *Biochemistry* **1993**, *32*, 11524-11529.
- (15) Lemieux, L. J.; Calhoun, M. W.; Thomas, J. W.; Ingledew, W. J.; Gennis, R. B. *J. Biol. Chem.* **1992**, *267*, 2105-2113.
- (16) Minagawa, J.; Mogi, T.; Gennis, R. B.; Anraku, Y. *J. Biol. Chem.* **1992**, *267*, 2096-2104.
- (17) *J. Biol. Chem.* **1994**, *269*, 11912-11920.
- (18) Thomas, J. W.; Calhoun, M. W.; Lemieux, L. J.; Puustinen, A.; Wikström, M.; Alben, J. O.; Gennis, R. B. *Biochemistry* **1994**, *33*, 13013-13021.
- (19) Uno, T.; Mogi, T.; Tsubaki, M.; Nishimura, Y.; Anraku, Y.; *J. Biol. Chem.* **1994**, *269*, 11912-11920.
- (20) Tsubaki, M.; Mogi, T.; Hori, H.; Hirota, S.; Ogura, T.; Kitagawa, T.; Anraku, Y. *J. Biol. Chem.* **1994**, *269*, 30861-30868.
- (21) Lemon, D. D.; Calhoun, M. W.; Gennis, R. B.; Woodruff, W. H. *Biochemistry* **1993**, *32*, 11953-11956.
- (22) Hirota, S.; Mogi, T.; Ogura, T.; Hirano, T.; Anraku, Y.; Kitagawa, T. *FEBS Lett.* **1994**, *352*, 67-70.
- (23) (a) Wang, J.; Ching, Y.-c.; Rousseau, D. L.; Hill, J. J.; Rumbley, J.; Gennis, R. B. *J. Am. Chem. Soc.* **1993**, *115*, 3390-3391. (b) Wang, J.; Ching, Y.-c.; Takahashi, S.; Gennis, R. B.; Rousseau, D. L. *Biochemistry* **1995**, *34*, 15504-15511.
- (24) Argade, P. V.; Ching, Y.-c.; Rousseau, D. L. *Science* **1984**, *225*, 329-331.
- (25) Yoshikawa, S.; Caughey, W. S. *J. Biol. Chem.* **1992**, *267*, 9757-9766.
- (26) Tsubaki, M. *Biochemistry* **1993**, *32*, 174-182.
- (27) Tsubaki, M.; Mogi, T.; Anraku, Y.; Hori, H. *Biochemistry* **1993**, *32*, 6065-6072.
- (28) Little, R. H.; Cheesman, M. R.; Thomson, A. J.; Greenwood, C.; Watmough, N. J. *Biochemistry* **1996**, *35*, 13780-13787.
- (29) Vygodina, T. V.; Konstantinov, A. A. *Biol. Membr.* **1985**, *2*, 861-869.
- (30) Li, W.; Palmer, G. *Biochemistry* **1993**, *32*, 1833-1843.
- (31) Tsubaki, M.; Mogi, T.; Hori, H.; Sato-Watanabe, M.; Anraku, Y. *J. Biol. Chem.* **1996**, *271*, 4017-4022.
- (32) Morgan, J. E.; Verkhovsky, M. I.; Wikström, M. *J. Bioenerg. Biomembr.* **1994**, *26*, 599-608.
- (33) Babcock, G. T. In *Biological Applications of Raman Spectroscopy*; Spiro, T. G., Ed.; Wiley: New York, 1988; Vol. 3, p 293.
- (34) Asher, S. A.; Vickery, L. E.; Schuster, T. M.; Sauer, K. *Biochemistry* **1977**, *16*, 5849-5855.
- (35) Asher, S. A.; Schuster, T. M. *Biochemistry* **1979**, *18*, 5377-5382.
- (36) Desbois, A.; Lutz, M.; Banerjee, R. *Biochemistry* **1979**, *18*, 1510-1515.
- (37) Tsubaki, M.; Srivastava, R. B.; Yu, N.-T. *Biochemistry* **1979**, *18*, 946-952.

- (38) Czernuszewicz, R. S.; Wagner, W.-D.; Ray, G. B.; Nakamoto, K. *J. Mol. Struct.* **1991**, *242*, 99–117.
- (39) Hill, J. J.; Goswitz, V. C.; Calhoun, M.; Garcia-Horsman, J. A.; Lemieux, L.; Alben, J. O.; Gennis, R. B. *Biochemistry* **1992**, *31*, 11435–11440.
- (40) Bormett, R. W.; Asher, S. A.; Larkin, P. J.; Gustafson, W. G.; Ragunathan, N.; Freedman, T. B.; Nafie, L. A.; Balasubramanian, S.; Boxer, S. G.; Yu, N.-T.; Gersonde, K.; Noble, R. W.; Springer, B. A.; Sligar, S. G. *J. Am. Chem. Soc.* **1992**, *114*, 6864–6867.
- (41) Bogumil, R.; Hunter, C. L.; Maurus, R.; Tang, H.-L.; Lee, H.; Lloyd, E.; Brayer, G. D.; Smith, M.; Mauk, A. G. *Biochemistry* **1994**, *33*, 7600–7608.
- (42) Blackburn, N. J.; Reedy, B.; Zhou, E.; Carr, R.; Benkovic, S. J. *J. Inorg. Biochem.* **1992**, *47*, 8–16.